A UAV-mounted THz spectrometer for real-time gas analysis

J.R. Demers*[a], F. Garet[b], and J.-L. Coutaz[b]
[a] Bakman Technologies LLC, 15462 Longbow Dr. Sherman Oaks, CA, USA 91403
[b] IMEP-LAHC, Université Savoie Mont Blanc, 73376 Le Bourget du Lac Cedex, France

ABSTRACT

A modified Bakman Technologies PB7200-2000-T portable THz spectrometer mounted to a consumer drone was employed to measure water vapor absorptions ten meters above the ground.

Keywords: Atmospheric Sensing**,** Unmanned Aerial Vehicle (Drone), Terahertz Spectroscopy, Photomixing, D_2O

1. INTRODUCTION

Terahertz (THz) spectroscopy is a useful tool for gas analysis because rovibrational transitions for a large variety of molecules occur in this frequency domain. These transitions are very specific to each molecule and under the right conditions may be used to measure the presence and concentration of different molecules in a gas sample. THz fingerprints are unique for several molecules of interest (like volatile organic molecules [1]) that cannot be detected or monitored in other domains of the electromagnetic spectrum (VIS, IR…). Moreover, in the THz range, absorption lines are less broadened by the Doppler effect and thus the spectral selectivity is better than in VIS or IR. Finally, THz spectroscopy is less sensitive to fog, smoke or dust in the atmosphere.

While a significant effort has been made to prove the ability of a laboratory based frequency domain THz spectroscopy to quantify different gases, for example the constituents of cigarette smoke [2], very little has been done in the field regarding atmosphere. X.-C. Zhang and his team [3] have demonstrated the possibility of identifying substance at a long remote distance using air breaking THz generation and several methods of detection (THz induced second harmonic generation, acoustic waves or fluorescence). These techniques require a powerful amplified femtosecond laser system. Another solution is to address molecular excitation at THz frequencies is to employ the Raman LIDAR technique [4], in which one records the Raman light backscattered by atmosphere up to several kilometers from the laser source. However, Raman scattering delivers a signal proportional to the derivative of the molecule polarizability with respect to the vibrational coordinates, while THz spectroscopy gives directly this polarizability. Thus the two techniques are complementary, but the THz spectra are often easier to interpret. Moreover, Raman LIDAR is mostly used to map only water vapor or ozone concentration, as well as atmospheric temperature [5] and suffers from the aspect that the response along the entire path is measured.

The lack of in-the-field THz spectroscopy can be explained by very significant challenges to producing a portable THz spectrometer which has the required spectral purity, frequency accuracy and detection sensitivity that would allow it to detect and quantify different molecules. If these challenges could be addressed, it would then be possible to perform in-situ measurements of atmosphere, especially where a direct remote observation is not possible, because of distance, obstructions or atmospheric conditions. We have previously reported on the first in-situ study of water vapor concentrations in atmosphere using a modified Bakman Technologies PB7220-2000-T THz spectrometer attached to a drone (Fig. 1) [6]. In that article, we also discussed the limitations in the spectral purity, frequency accuracy and detection sensitivity that limited the performance. Here, we discuss the advancements that we have made to address the shortcomings of the instrument, primarily the addition of a lightweight, low-pressure sample cell and a balanced photo-mixing architecture.

Figure 1. The modified PB7220-2000-T air-born and collecting data roughly 10 meters above the ground.

2. INSTRUMENTATION AND METHODOLOGY

As with the previously reported experiment, we employed a PB7220 portable frequency domain THz spectrometer from Bakman Technologies (Fig 2). The spectrometer employs a pair of wavelength offset 783 nm, temperature tunable, DFB lasers the 40 mW outputs of which are coupled into a 2×2 phase maintaining (PM) splitter. One of the splitter outputs is fiber coupled into the center of an antenna sputtered onto a LTG GaAs substrate. A 6-kHz, 20-V peak-to-peak square wave bias is applied to the antenna and this photomixer radiates the modulated laser difference frequency. Sweeping the THz frequency is accomplished by temperature tuning the lasers relative to each other. The second splitter output is fiber coupled to a similar photomixer, but instead of biasing the antenna, it is directly connected to a trans-impedance amplifier (TIA) which in turn is connected to a lock-in amplifier. The THz radiation from the source is coupled to free space via a Si lens attached to the LTG GaAs substrate. The beam is collimated with an off axis parabolic mirror and sent through the plastic window of a 75 cm, carbon fiber sample cell in which the pressure can be varied between 760 Torr and 1 Torr with a micro scroll pump. The combined mass of the sample cell and pump is 0.75 kg. It is worth noting that the radiation propagates through roughly 6 cm of atmosphere at standard pressure and temperature on each side of the sample cell. The sample pressure is monitored with an analog pressure gauge attached to the same vacuum line as the sample bottle and the pressure is controlled with a needle valve on the micro-pump. Liquid samples are placed in the sample bottle. After passing through the sample cell, the THz radiation is coupled through a Si lens and onto the detection photomixer.

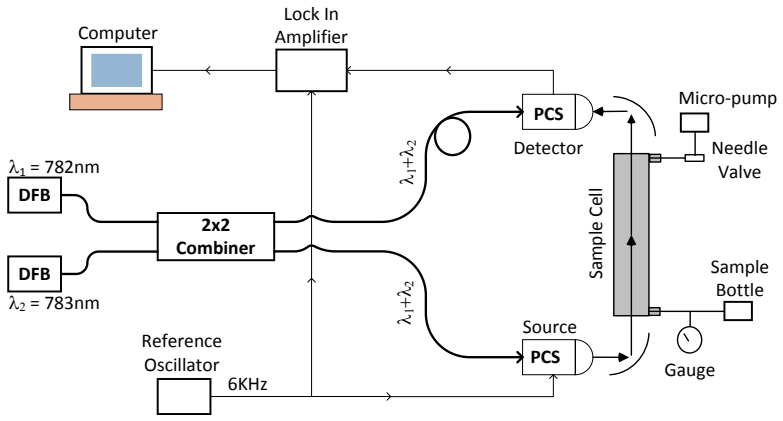

Figure 2. A schematic of the instrument and sample cell employed for these measurements.

This instrument employs homodyne detection. While this dramatically improves the dynamic range of the instrument,

it does have a significant drawback: it results in a 'fringe pattern' that occurs as the detected THz radiation and the local THz radiation come into and out of phase relative to each other [7]. This fringe pattern can be seen at the bottom of the plot in Fig. 3 which is the previously reported spectrum of atmosphere recorded 10-m above ground [6]. The upper trace is a plot of the maximums of the fringes and illustrates spectral features of water vapor but at a great expense to resolution and SNR. The spectral resolution is indeed given by the fringe spacing, while the depth of the absorption lines is determined with a precision equal to the signal amplitude difference between fringe maximum and minimum at the resonances.

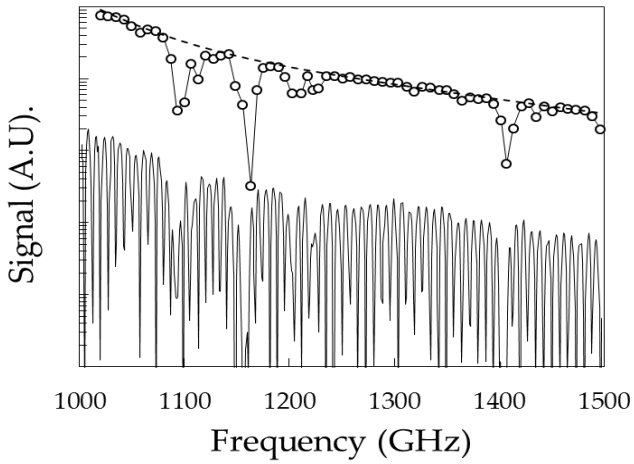

Figure 3. Raw spectrum (lower curve) and extracted fringes maxima (upper curve) of atmosphere recorded 10-m above ground. For the sake of legibility, the two curves have been vertically shifted by ×50. The dashed line is a fit of the out-of-resonance filtered data, i.e. it corresponds to the baseline of the signal.

However, the issues due to the fringes can be minimized by adjusting the optical fiber length to the detector such that it is approximately equal to the fiber length to the source plus approximately half the THz beam path length (fiber index is greater than air index). The separation between the source and detection heads may then varied in slight increments to 'balance' the system such that any remaining fringes fall outside of the spectral region of interest. This condition is illustrated in Fig. 4 where, along with a water vapor line at 1410 GHz, the spectrum shows a fringe at 1320 GHz.

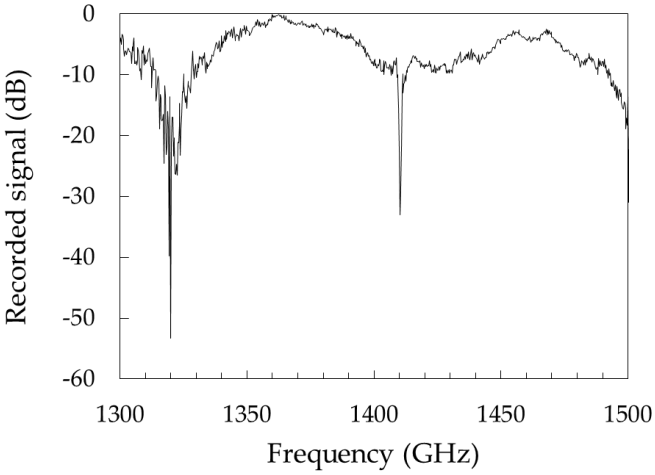

Figure 4. A spectrum showing the 1410 GHz water vapor transition (30 Torr with 250 MHz resolution) and a fringe due to homodyne detection at 1320 GHz.

3. EXPERIMENTAL RESULTS

3.1 Drone experiment

We first treat the spectrum of atmosphere (Fig. 3) recorded with the drone-mounted system. The absorption coefficient is determined by inverting expression $T(\omega) = e^{-\alpha(\omega)L}$, assuming the maximum of transmission of the available experimental spectrum $T(\omega)$, as regards to the fitting baseline, is equal to 1 (upper curve in Fig. 3). The absorption spectrum is plotted in Fig. 5 (left). For comparison, the absorption spectrum predicted by Slocum *et al.* [8], for two different humidity percentages (50 and 81%), are plotted on the same figure. The agreement between values extracted from the drone measurement and predicted ones is excellent (note that the vertical scale is logarithmic), especially if one takes into account the spectral resolution of the experiment, as well as the noise level (which forbids here to determine α below 4~5×10^{-3} cm^{-1}). According to the modeling by Slocum *et al.*, α varies almost linearly with the humidity level. The 81% plot corresponds to the best fit of the experimental data using the model by Slocum *et al*. This humidity percentage (81% ± 15%) was obtained by adjusting the calculated value of α with the measured one at 1185 GHz (Fig. 5 right). We especially selected this frequency because: 1) at this value, the absorption spectrum shows a broad minimum that is not perturbed by the experimental frequency resolution; 2) this minimum (α~0.01 cm^{-1}) is largely over the noise level.

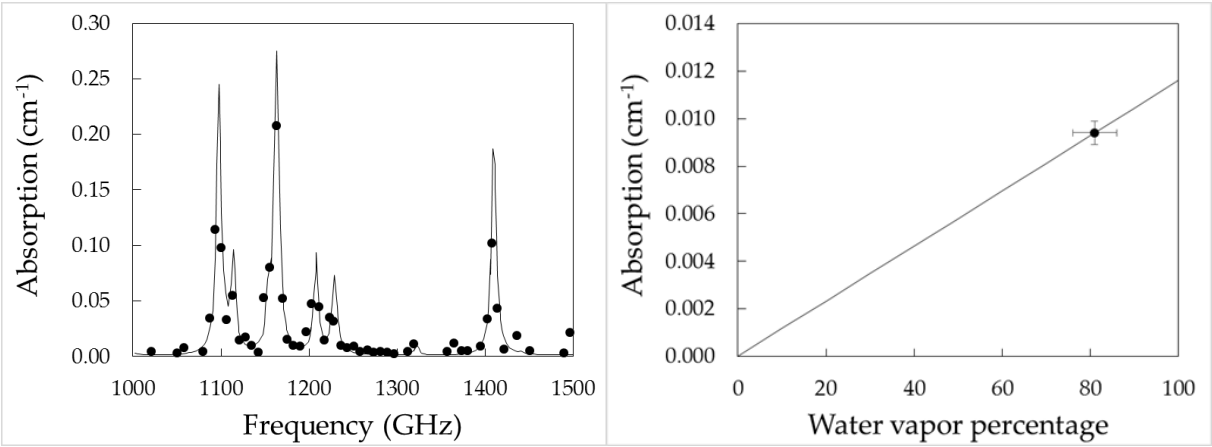

Figure 5. Left: Atmosphere absorption spectrum recorded 10-m above ground. Full circles are values deduced from the drone measurement and continuous line is a theoretical curve calculated from [9] for 81% of humidity. The choice of the 81% value is evinced on the right-side plot given for 1185 GHz (line: theoretical curve calculated from [9], full circle: experimental data).

3.2 $H_2O/D_2O/HDO$ experiments

This set of experiments, performed in the laboratory, aim at evaluating the sensitivity and spectral resolution of the spectrometer. We study natural spring water (Evian), and heavy water (both D_2O and HDO). In this work, the cell is made empty (p < 10 Torr), then the bottle containing the liquid sample is opened and its vapor fills the cell. Fig. 6 shows the recorded spectra of the empty cell and the D_2O vapor. The vapor pressure is 50 Torr and the data are recorded every 250 MHz. Fig. 6 left shows the recorded signals (log scale) and Fig. 6 right presents the absorption of D_2O (open circles) determined from the experimental curves (left side). The continuous curve is calculated from the JPL database [9], assuming a Lorentzian shape for each resonance. The agreement between experimental data and the JPL database curve is very good. Let us notice that here the only adjustable variable is the Lorentzian resonance width Δf, that for the sake of simplicity, we set constant for each resonance. The best fit is obtained with Δf = 1.2 GHz. Let us examine the 1410 GHz line, which corresponds to the rotational transition $J'_{K'_aK'_c} = 5_{2,3} \rightarrow J_{K_aK_c} = 5_{1,4}$ [10]. The line with of absorption peaks of a gas is indeed proportional to the pressure and temperature ($\Delta f = \gamma P$, where γ is the pressure broadening parameter). In air at atmospheric pressure, the line broadening is due to the collisions between molecules, while the

Doppler effect broadening is negligible (of the order of MHz) [11]. The value, deduced from the record, of the pressure broadening parameter γ for the 1410-GHz line is $\gamma = \frac{\Delta f}{P} \approx 180$ MHz/kPa. This value is about 6 times bigger than those reported by Hoshina *et al.* [10] for broadening of water vapor in N_2 or in O_2. However, self-broadening of water vapor in the THz range is known [12] to lead to 5~6 times larger line widths than broadening with N_2, which is in accordance with our observation. As expected, the line width decreases down to 750 MHz under a 30-Torr pressure and to 250 MHz at 10 Torr. This last line width value corresponds to the spectral interval between two neighboring recorded points. Fig. 7 (left) presents this recorded 1410 GHz line of H_2O vapor at 10 Torr. Here again, the agreement between measured data and the JPL database curve, calculated with Δf = 250 MHz, is excellent.

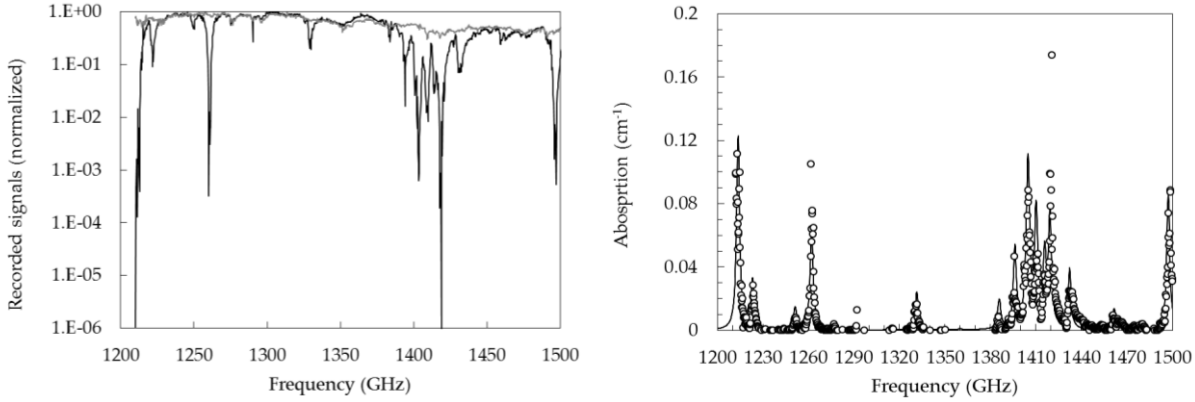

Figure 6. Left: Recorded signals versus frequency for the empty cell (grey line) and the cell filled with D_2O vapor at a pressure of 50 Torr (black line). Right: Absorption of D_2O vapor determined from the measured signals (open circles) and calculated from the JPL database (continuous curve).

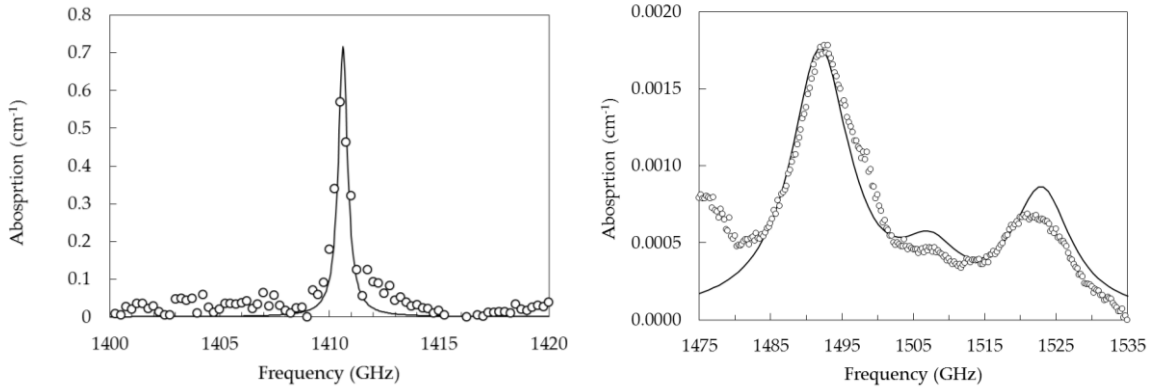

Figure 7. Left: Absorption of H_2O vapor around 1410 GHz determined from the measured signals (open circles) and calculated from the JPL database (continuous curve). Right: the same for HDO.

Another example is given on Fig. 7 (right): 3 absorption lines of HDO at STP around 1.5 THz are shown with a resolution of 250 MHz and a 10 scan average.

4. FUTURE WORK

While we have shown that it is possible to 'work around' the fringes, the method of adjusting lengths may be acceptable for laboratory measurements, but it is not for autonomous measurements in real environments with significant temperature changes. Nor will this method be suitable when gas mixtures are being studied since fringes will invariably cover important spectral features. Also, the shifting of the positions of the fringes during averaging made it very difficult

to create a reliable and repeatable baseline and resulted in poor averaging and significant degradation of SNR. We plan to perform careful laboratory measurements to determine the system sensitivity for atmospheric gases of importance, but because of the issues with the fringes, these measurements will have to wait until we employ our previously reported all-optical technique for removing the fringes [13-15]. We plan to employ the same architecture (Fig. 8) for our next drone spectrometer along with a 1 meter, multipath cell (effective 10 meter) to increase system sensitivity.

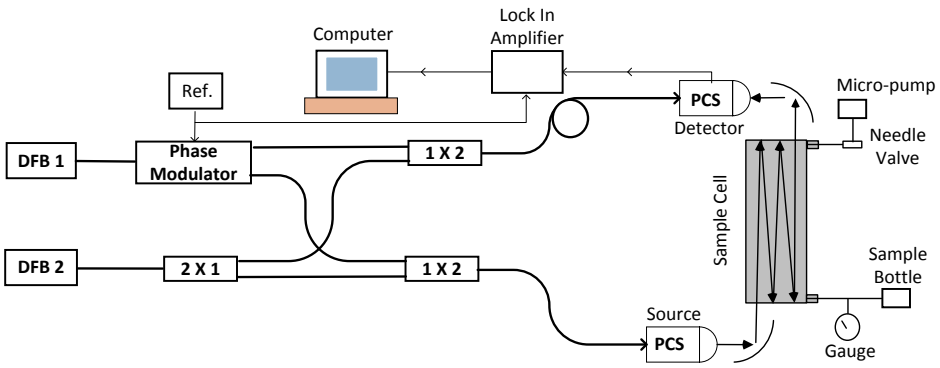

Figure 8. Future spectrometer with phase control for fringe suppression and a multipath cell for increased sensitivity.

5. CONCLUSIONS

We have reported on the progress made towards a portable, high-resolution, photomixing THz spectrometer small enough to be carried on a drone but with the potential required for measuring concentrations of atmospheric gases of importance. The system was employed to measure H_2O and D_2O lines at pressures of less than 10 Torr with a sample cell and pump that together weighed less than 0.75 kg.

ACKNOWLEDGMENTS

This project has been partially funded by the National Science Foundation, USA. We would like to thank the University of Savoie Mont Blanc, which provided some support for Dr. Demers collaborative visit. We would also like to thank Mr. Edan Cain and Cheetah Logistics of Westlake, CA for providing and piloting the DJI-S1000, Mr. Jacob Christ of ProLinear/PONTECH for software support, Mr. Thomas Logan and Dr. Ronald T. Logan, Jr.

REFERENCES

[1] Hindle F, Cuisset A, Bocquet R, and Mouret G (2008), "Continuous-wave terahertz by photomixing: applications to gas phase pollutant detection and quantification," *C. R. Physique*, vol. 9, pp. 262-275.

[2] Bigourd D, Cuisset A, Hindle F, Matton S, Fertein E, Bocquet R, and Mouret G (2006), "Detection and quantification of multiple molecular species in mainstream cigarette smoke by continuous-wave terahertz spectroscopy," *Opt. Lett.*, vol. 31, pp. 2356-2358.

[3] Clough B and Zhang X-C (2014), "Toward remote sensing with broadband terahertz waves," *Front. Optoelectron.*, vol. 7, pp. 199-219.

[4] Nedeljkovic N, Hauchecorne A, and Chanin M L (1993), "Rotational Raman lidar to measure the atmospheric temperature from the ground to 30 km," *IEEE Trans. Geoscience and Remote Sensing*, vol. 31, pp. 90-101.

[5] Marc M, Tobiszewski M, Zabiegała B, de la Guardia M, and Namiesnik J (2015), "Current air quality analytics and monitoring: A review," *Anal. Chim. Acta*, vol. 853, pp. 116-126.

[6] Demers J R, Garet F and Coutaz, J-L (2017), "Atmospheric water vapor absorption recorded ten meters above the ground with a drone mounted frequency domain THz spectrometer," *IEEE Sensors Letters*, vol. 1, pp. 1-3.

[7] Demers J R, Logan Jr. R T, Bergeron N J, and Brown E R (2008), "A coherent frequency-domain THz spectrometer with a signal-to-noise ratio of 60 dB at 1 THz," in *Terahertz for Military and Security Applications VI* (SPIE Proc. 6949), p. 694909; DOI:10.1117/12.777457.

[8] Slocum D M, Slingerland E J, Giles R H, and Goyette T M (2013), "Atmospheric absorption of terahertz radiation and water vapor continuum effects," *J. Quant. Spectrosc. Radiat. Transfer,* vol. 127, pp. 49-63.

[9] https://spec.jpl.nasa.gov/.

[10] Hoshina H, Seta T, Iwamoto T, Hosako I, Otani C, and Kasai, Y (2008), "Precise measurement of pressure broadening parameters for water vapor with a terahertz time-domain spectrometer," *J. Quant. Spectro. Rad. Transfer*, vol. 109, pp. 2303-2314.

[11] Atomic, Molecular, & Optical Physics Handbook, ed. by G.W.F. Drake (AIP, Woodbury, NY, 1996).

[12] Cazzoli G., Puzzarini C., Buffa G., and Tarrini O. (2008), "Pressure-broadening of water lines in the THz frequency region: Improvements and confirmations for spectroscopic databases," *J. Quant. Spectrosc. Radiat. Transfer*, vol. 109, pp. 2820–2831.

[13] Demers J R, and Kasper B L (2013), "Employing phase modulation and second harmonic nulling to eliminate the interference fringes from the spectrum of a portable coherent frequency-domain THz spectrometer," in *Terahertz Physics, Devices, and Systems* VII (SPIE Proc. 8716), p. 87160M.

[14] Demers J R, and Kasper B L, "Phase modulation and second-harmonic nulling to eliminate interference fringes from the spectrum of a coherent frequency-domain THz spectrometer," in *Proc. of 38th International Conference on Infrared, Millimeter, and Terahertz Waves* (IRMMW-THz 2013), DOI: 10.1109/IRMMW-THz.2013.6665794.

[15] Demers J R, Kasper B, and Daughton D R, "Simultaneous measurement of the 1st and 2nd harmonics of a phase modulated coherent frequency-domain THz spectrometer," in *Proc. of 39th International Conference on Infrared, Millimeter, and Terahertz Waves* (IRMMW-THz 2014), DOI: 10.1109/IRMMW-THz.2014.6956079.